ELSEVIER

PII: S0032-3861(97)00222-X

Polymer Vol. 39 No. 10, pp. 1779–1785, 1998

0032-3861/98/$19.00+0.00

Blends of poly(vinylidene fluoride) with polyamide 6: interfacial adhesion, morphology and mechanical properties

Z. H. Liu, Ph. Maréchal and R. Jérôme*
Center for Education and Research on Macromolecules, University of Liège, Sart-Tilman, B6, 4000Liège, Belgium
(Received 3 September 1996)

The poly(vinylidene fluoride) (PVDF)/polyamide 6 (PA6) interfacial adhesion has been measured, and morphology and mechanical properties of the binary blends have been investigated. The lap shear strength of the PVDF/PA6 pair indicates a high interfacial adhesion, which is evidence for specific intermolecular interactions between the two polymers. Immiscibility of PVDF and PA6 has clearly been observed by transmission electron microscopy (TEM). It reflects the high propensity of each polymer to crystallize on its own and the strong hydrogen bonding that prevails in PA6. This interfacial adhesion can account for the fine phase morphology of the binary blends. Dependence of Young's modulus and yield stress on the blend composition shows a slightly negative deviation with respect to the additivity law, in contrast to elongation at break, ultimate tensile strength and impact toughness that display a positive deviation. These experimental observations have been discussed in reference to the interfacial adhesion and the change in crystallinity of the continuous phase. An optimum interfacial adhesion seems to be required for promoting a synergism in the impact resistance of these polyblends.

(Keywords: interfacial adhesion; phase morphology; synergism)

INTRODUCTION

Poly(vinylidene fluoride) (PVDF) is a very useful thermoplastic that combines an excellent chemical resistance[1] with ferroelectric, piezoelectric and pyroelectric properties[2–4]. A high cost is however a limitation for widespread applications. Today, polymer blending is a versatile and widely used method for optimizing the cost-performance balance and increasing the range of potential applications.

Miscibility and mechanical properties of PVDF/poly(methylmethacrylate) (PMMA) blends have been extensively studied[5–9]. These blends are valuable models for miscible semi-crystalline polymer/amorphous polymer blends. Actually, PVDF and PMMA are completely miscible in the melt[5], and phase separation occurs upon cooling as a result of PVDF crystallization in a close relationship with blend composition and cooling conditions[6,7]. These blends are, however, quite brittle, as shown by Mizovic et al.[8] who reported that the impact strength dramatically decreased when the PMMA content was increased. Murff et al.[9] have observed a negative deviation in the ultimate tensile strength composition relationship of the PVDF/PMMA blends.

Special attention has also been paid to blends of PVDF with immiscible polymers, and strategies have been devised to improve the detrimental effect of polymer immiscibility on the mechanical properties. A series of blends of PVDF with, e.g. Noryl[10,11], poly(α-methylstyrene)[12] and polyolefins [polyethylene (PE) and polypropylene (PP)][13] have been added with diblock copolymers, i.e. poly(styrene b-methylmethacrylate)[10,11], poly(α-methylstyrene-b-methylmethacrylate)[12], and poly(hydrogenated diene-b-methylmethacrylate)[13], respectively, that have proved to be very efficient interfacial agents. Siqueira and Nunes[14] have investigated the compatibilizing capability of styrene and methylmethacrylate random and block copolymers in PVDF/PS blends. Deleens et al.[15,16] have used poly(ether-amide) block copolymers as compatibilizers in the immiscible PVDF and PA12 polyblends. Since the availability of block copolymers on the market place is usually a problem, blends of immiscible polymers with favourable interfacial interactions might be an alternative. In this regard, polyamide 6 (PA6) might be a valuable candidate for blending with PVDF. Indeed, some amide containing small organic molecules, e.g. N, N-dimethylacetamide (DMAC) and N, N-dimethylformamide (DMF), are solvents for PVDF although PVDF is essentially insoluble in most organic solvents[17]. This suggests that there may be specific intermolecular interactions between PVDF and the amide containing solvents. This effect has been recently confirmed in the case of ϵ-caprolactam[16]. Furthermore, an increase in the content of the interacting groups is expected to improve the polymer compatibility and, accordingly, the interfacial adhesion, as would be the case for the substitution of PA6 for PA12. This effect has been convincingly illustrated by the poly(vinyl chloride) (PVC)/poly(butadiene-co-acrylonitrile) (NBR) blends. Indeed, polymer miscibility is improved when the acrylonitrile content of the NBR rubber is increased[19,20].

This paper aims at reporting on the interfacial adhesion between PVDF and PA6 as measured by the lap shear strength. Attention will also be paid to the effect of the

* To whom correspondence should be addressed

Table 1 Polymers used in this study

Polymer	Commercial designation	Molecular weight	Source
Poly(vinylidene fluoride)	Solef 1008	Mn = 39 000	Solvay
Polyamide 6	Ultramid B4	Mn = 33 000	BASF
		Mn = 110 000	
Poly(methylmethacrylate)	Diakon	Mn = 45 000	I.C.I.
Polystyrene		Mn = 158 000	BASF
Polypropylene	S306		Molpen

interfacial adhesion on the phase morphology and mechanical properties of the PVDF/PA6 blends.

EXPERIMENTAL

Molecular weight and origin of the polymers used in this study are reported in *Table 1*. PA6 and PVDF/PA6 blends were dried in a vacuum oven at 125°C for two days prior to melt processing, in order to avoid the PA6 hydrolysis by residual water.

Sandwiches of polymer A-polymer B-polymer A were prepared by compression molding under a pressure of 20 kg/cm^2 for 10 min, at various temperatures. Thickness of polymer A and polymer B layers was 2 mm and 1 mm, respectively. The lap shear strength was measured according to ASTM D1002 with a tensile testing machine at a cross-head speed of 5 mm/min at room temperature.

PVDF and PA6 were melt blended in a Brabender internal mixer at 240°C and a screw speed of 30 rpm for 15 min. Then, they were compression-molded into sheets of a thickness of 2 mm and 4 mm, respectively.

Morphology of the PVDF/PA6 blends was observed with a Phillips CM100 transmission electron microscope (TEM). Ultramicrotomed samples were treated with a 2 wt% aqueous solution of phosphotungstic acid at 60°C in order to stain selectively the PA6 phase.

Standard tensile specimens were machined from the 2-mm-thick sheets. They were tested according to ASTM D638 at a cross-head speed of 5 mm/min at room temperature. Young's modulus, yield stress, elongation at break and ultimate tensile strength were accordingly measured. Charpy impact strength was measured at room temperature according to ASTM D256 ('U' notch), with samples machined from the 4-mm-thick sheets and a Charpy CEAST 6546 apparatus.

RESULTS AND DISCUSSION

Lap shear strength

Measurement of the lap shear strength is a straightforward way to estimate the adhesion between two immiscible polymers. This property indeed depends on polymer–polymer interactions (thermodynamic contribution) and any parameters that control kinetics of the polymer chain interdiffusion, such as temperature, time and pressure (kinetic contribution). Roughness and contamination (or not) of the joined surfaces is also of prime importance[21]. The lap shear strength between identical or miscible polymers can be very high, since polymer chain segments can interpenetrate across the interface with formation of an interfacial layer of at least one entanglement mesh size and with substitution of a cohesive failure for the less desirable interfacial fracture[22].

The lap shear strength of a series of polymer pairs has been measured as reported in *Table 2*, with the purpose of comparing the PVDF/PA6 interfacial adhesion with pairs of miscible polymers (PVDF/PMMA) and pairs in which PVDF has no specific intermolecular interactions with the second polymer, i.e. PVDF/polystyrene (PS) and PVDF/polypropylene (PP). Polymer sheets were assembled face-to-face and compressed under the same pressure, for the same period of time, at various temperatures. *Table 2* confirms that a high interfacial adhesion can be expected for a miscible polymer pair provided that the mutual interdiffusion of chain segments of each polymer occurs to a large enough extent. The lap strength of the PVDF/PMMA/PVDF system is indeed zero when compressed at 140°C for 10 min under 20 kg/cm^2. Under the same experimental conditions, the interfacial adhesion grows up to 21 MPa when the compression temperature is increased by 20°C, thus up to 160°C. It is worth recalling that the lower critical solution temperature for the PVDF/PMMA pair is at least 330°C under atmospheric pressure[5]. In agreement with the PVDF/PS immiscibility[14], the lap strength measured for the PVDF/PS/PVDF system is zero even at a compression temperature as high as 180°C, thus above the PVDF melting temperature (177°C)[23] and the PS glass transition temperature (*ca.* 100°C)[24]. These results are consistent with observations reported in the scientific literature[25]. So, at a compression molding temperature of 160°C, diffusion into the PVDF matrix can occur under the experimental conditions used in this work. These conditions allow to discriminate PS and PMMA, i.e. two amorphous polymers of a Tg below 160°C, in terms of miscibility toward PVDF. PA6 and PP are also known for complete immiscibility as supported by data in *Table 2*. Substitution of PVDF for PP is very interesting, since in the same compression temperature range (220–230°C), an interfacial adhesion is now measured (*Table 2*). This adhesion, however, rapidly exceeds the mechanical resistance of the outer PA6 layer, which prevents it being quantitatively measured.

Table 2 Lap shear strength for miscible and immiscible polymer pairs[a]

System	Pressing temperature (°C)	Average lap shear strength, MPa
PVDF/PMMA/PVDF	140	0
	160	21.0
PVDF/PS/PVDF	160	0
	180	0
PA6/PP/PA6	220	0
	230	0
PA6/PVDF/PA6	180	0
	220	7.0
	230	> 9.0[b]

[a] Contact time: 10 min; pressure 20 kg/cm^2. [b] Failure occurs in the PA6 outer layer for a shear strength of 9 MPa.

Compared to the PVDF/PS and PA6/PP interface, it is clear that the PVDF/PA6 interface is strengthened by specific intermolecular interactions between the two polymers which agrees with the solubility of PVDF in the melted ϵ-caprolactam[18], i.e. the cyclic monomer precursor of PA6.

Morphology

According to Wu[26], the number average size of the dispersed phases in binary blends (An) is proportional to the interfacial tension (γ) and the viscosity ratio of the dispersed phase to the continuous one (η_d/η_m) and inversely proportional to the shear rate (G) and melt viscosity of the matrix (η_m) [equation (1)].

$$\mathrm{An} = \frac{4(\eta_d/\eta_m)^k\gamma}{G\eta_m} \quad (1)$$

where $k = 0.84$ for $\eta_d/\eta_m \geq 1$; $k = -0.84$ for $\eta_d/\eta_m \leq 1$.

PVDF/PA6 blends have been melt blended at 240°C in an internal mixer. *Figure 1* shows the composition dependence of the relative torque, i.e. torque of the blend compared to PA6. At 240°C, the torque and thus the melt viscosity of PVDF is *ca.* half the value reported for PA6. A positive deviation of the relative torque with respect to the linear relationship (dotted line in *Figure 1*) is observed, whereas in the composition range of more than 35 wt% PA6, the torque of the blend exceeds the torque of each constitutive component, which is known as synergism. This positive deviation may be indicative of interactions between the blended polymers[27].

Blend morphology has been observed by TEM, and the phase contrast has been enhanced by the selective staining of PA6 by phosphotungstic acid (PA6 is then observed as a dark phase). *Figure 2*a–e shows the micrographs of blends containing 20, 40, 50, 60 and 80 wt% PA6, respectively. In blends containing less than 50 wt% PA6, PVDF is the continuous phase (*Figure 2*a and b), and the average size of the dispersed PA6 phases ranges from 0.1 μm and 1 μm, depending on the blend composition. At a composition of 50 wt% PA6 (*Figure 2*c), PA6 clearly forms a continuous phase and PVDF starts to be discontinuous, although a reliable conclusion on a 3-D morphology cannot be drawn from a 2-D observation, particularly for compositions close to the phase inversion. When PA6 is the major component, the average size of the PVDF domains decreases from *ca.* 0.5 μm to 0.1 μm when the PA6 content is increased. Thus,

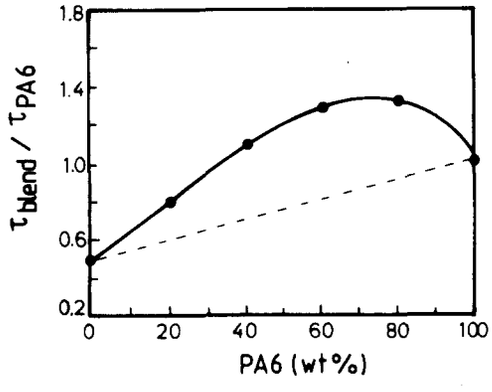

Figure 1 Relative torque (τ_{blend}/τ_{PA6}) versus composition for PVDF/PA6 blends. The torque (τ) was measured for 15 min of blending at 240°C and a screw speed of 30 rpm.

at the same content of the dispersed phase, PVDF forms smaller phases than PA6, in agreement with equation (1) and *Figure 1*. Indeed, all the blends have been prepared at a constant screw speed of 30 rpm (thus G constant) and η_m (that may be approximated to the torque[24]) is higher than η_d when PA6 is the continuous phase. Equation (1) accordingly predicts a smaller average size (An) for dispersed PVDF phases compared to PA6, which agrees with the experimental observations.

It is worth comparing, although on a qualitative basis, the average size of the dispersed phases in the PVDF/PA6 blends to values reported for two-phase binary blends containing either PA6 or PVDF as one constitutive component. As a rule, values larger than 4–5 μm have been reported for PP dispersed in PA6[28,29], and for dispersions of PP, Noryl, polystyrene (PS) or poly(α-methylstyrene) in PVDF[10–14]. Lap shear strengths in *Table 2* show that the interfacial adhesion between PA6 and PP, and PVDF and PS is negligible, in contrast to the value measured for the PVDF/PA6 pair. It can be inferred from these data that a comparatively lower interfacial tension in the PVDF/PA6 blends is in favour of a finer phase morphology compared to blends in which no specific cross-interaction occurs. In spite of favourable mutual interactions, PVDF and PA6 are immiscible, indicating that the PVDF/PA6 cross-interactions cannot match the PVDF-PVDF and the particularly strong PA6-PA6 interactions (H bonding).

The composition at which the relative melt viscosity goes through a maximum (or a minimum) is usually referred to as the composition of phase inversion. This composition can be approximated to *ca.* 75 wt% PA6 (*Figure 1*). This value is in complete disagreement with the observation of the phase morphology by TEM, which indicates that the phase inversion has already occurred (or at least is occurring) in blends containing 50 wt% PA6.

$$\frac{\eta_1}{\eta_2}\cdot\frac{\phi_1}{\phi_2} = 1 \quad (2)$$

Contradiction between TEM observations and torque measurements is not alleviated by reference to equation (2), which is an empirical relationship between the relative melt viscosity of PVDF (1) and PA6 (2), and the volume fraction of the phases at the phase inversion. On the assumption that the torque ratio may be substituted for the melt viscosity ratio, *Figure 1* shows that $\eta_1/\eta_2 = 0.51$. Then, it results from equation (2) that ϕ_{PA6} should be 0.33 at the phase inversion, which completely disagrees with both morphology and torque data. Failure of equation (2) to predict the phase inversion has already been reported[30], which suggests that experimental parameters other than melt viscosities have a decisive effect on the phase morphology.

Mechanical properties

Young's modulus of polymer blends mainly depends on the modulus of each constitutive component and blend composition. It is also somewhat affected by the interfacial interactions and changes in the phase morphology[31]. *Figure 3* shows that this general behaviour is not confirmed by the PVDF/PA6 blends that show a pronounced negative deviation with respect to the weight average values (dotted line).

An explanation for this observation might be found in a change in the crystallinity degree of the continuous phase as

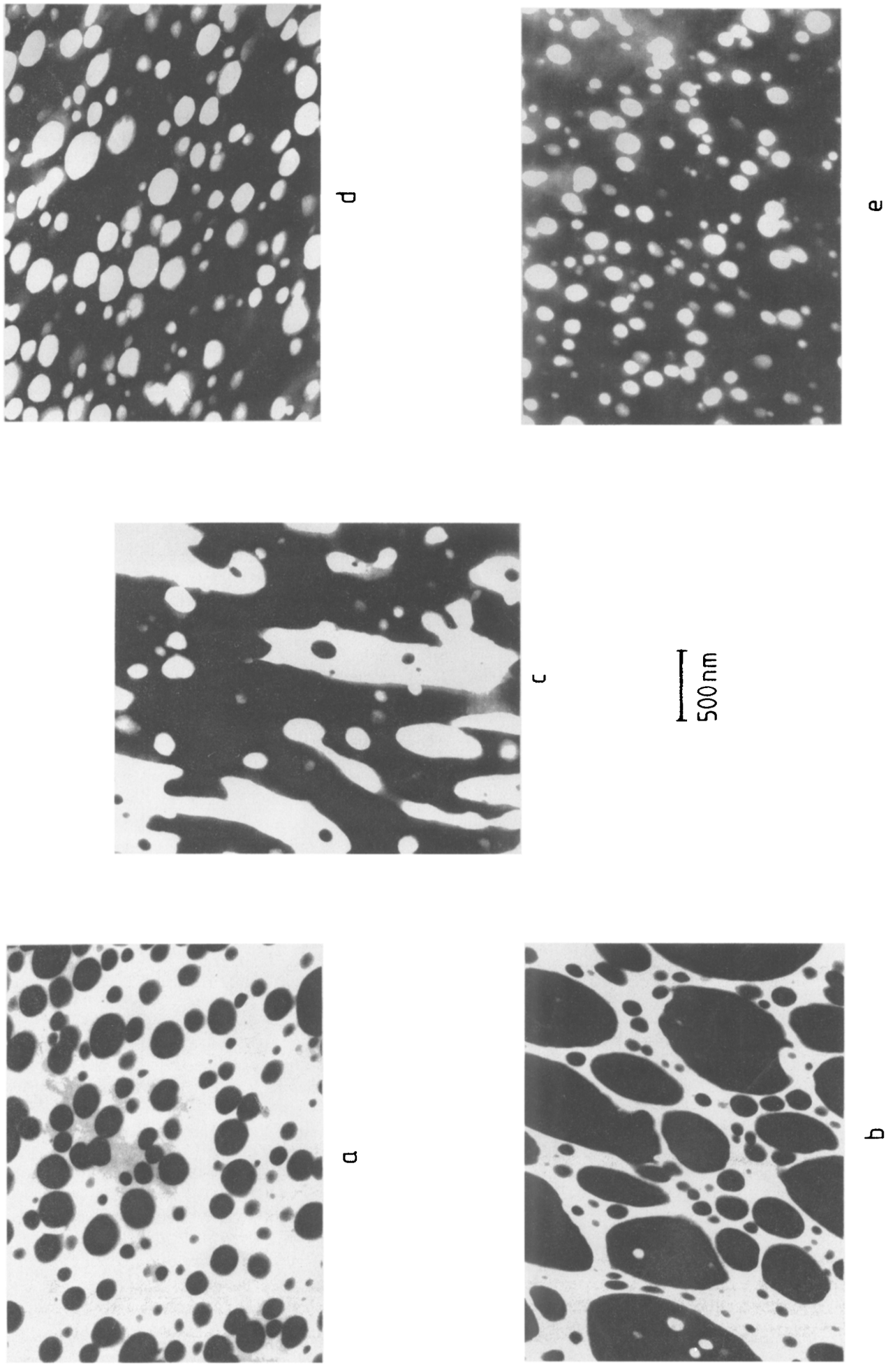

Figure 2 Transmission electron micrographs for PVDF/PA6 blends of various wt compositions. (a) 80/20, (b) 60/40, (c) 50/50, (d) 40/60, (e) 20/80. PA6 was stained with phosphotungstic acid (dark phase). The scale bar stands for 500 nm in all cases.

the blend composition is changed. The modulus of a semi-crystalline polymer is indeed expected to decrease with decreasing crystallinity. A previous study has shown that the PVDF crystallinity rapidly decreases upon addition of PA6 at least until 30 wt%[23], thus when PVDF is the continuous phase. In this particular composition range, the modulus drops rapidly. Beyond 30 wt% PA6, the crystallinity degree of PVDF tends to level off, and the two-phase system comes closer to phase inversion. This explains why a flat minimum is then observed in the composition dependence of the modulus before increasing up to the modulus of PA6. The comparatively less pronounced change in modulus when PA6 is the continuous phase is in line with the less sensitivity of the PA6 crystallinity on the PVDF addition compared to the reverse situation[23].

Figure 4 illustrates the yield stress–composition relationship for the PVDF/PA6 blends and a small negative deviation. Recent studies have suggested that the yield behaviour of polymer blends is affected by the interfacial adhesion[31,33,34,37]. Pukanszky et al.[31,32–37] have proposed the upper and lower values for the yield stress, in case of extreme values of interfacial adhesion. When the interfacial adhesion is strong enough for the stress transfer to occur between two phases, the yield stress would obey the law of mixtures (the upper value):

$$\sigma_{y,b} = \sigma_{y,1}\phi_1 + \sigma_{y,2}\phi_2 \qquad (3)$$

where σ_y is the yield stress and the subscripts b, 1 and 2 refer to blend, component 1 (PVDF) and component 2 (PA6), respectively.

In the case of lack of interfacial adhesion, dispersion of the minor component only results in a reduction of the load bearing cross-section of the matrix. The yield stress in then calculated by equation (4) [the lower value]

$$\sigma^0_{y,b} = \sigma_{y,m}\frac{1-\phi_d}{1+2.5\phi_d} \qquad (4)$$

where superscript '0' denotes a 'zero' interfacial adhesion, m is the matrix or the continuous phase, and d the dispersed phase. *Figure 5* compares the experimental data with the predictions for extreme interfacial adhesion. The ordinate of the plot is $\sigma_y/\sigma_{y,b}$, where σ_y stands for $\sigma_{y,b}$ when equation (3) is concerned (strong interfacial adhesion), for $\sigma^0_{y,b}$ when predictions of equation (4) are plotted (no interfacial adhesion) and for the experimental data (full line and full circles), respectively. The Pukanszky model gives credit to a strong interfacial adhesion between PVDF and PA6.

Figure 6 shows how the elongation at break depends on the PA6 content. A positive deviation is obvious and the elongation at break is higher than the values measured for each component in a large composition range (> 30 wt% PA6). The increase in the elongation at break is spectacular

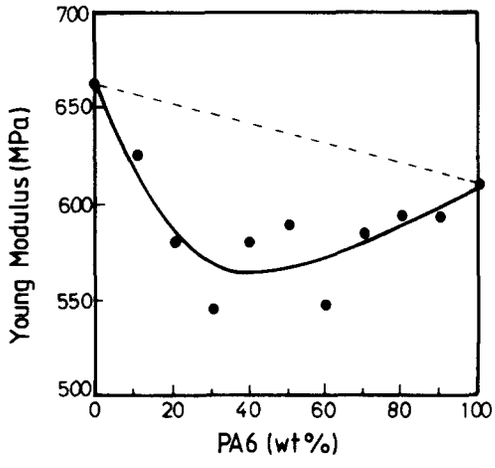

Figure 3 Young's modulus versus composition for PVDF/PA6 blends.

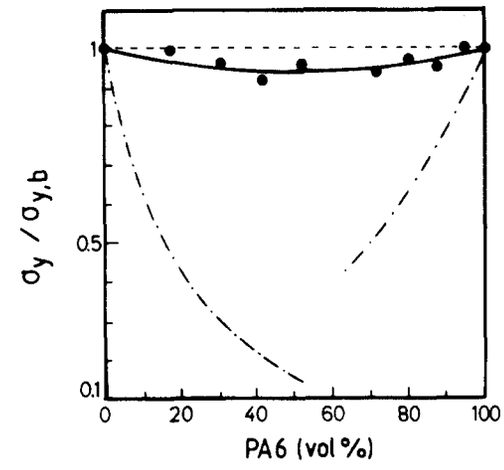

Figure 5 $\sigma_y/\sigma_{y,b}$ versus composition for PVDF/PA6 blends. Comparison of experimental data (●) and values calculated by equations (3) (- - - -) and (4) (·····), respectively.

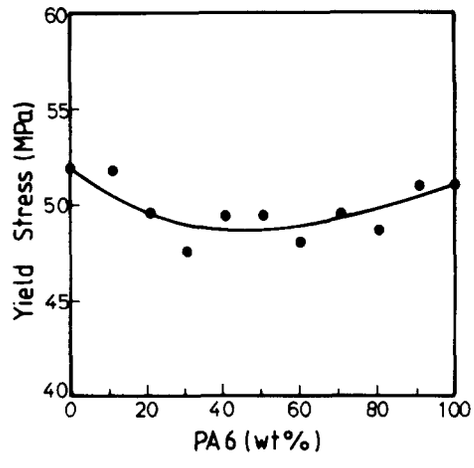

Figure 4 Yield stress versus composition for PVDF/PA6 blends.

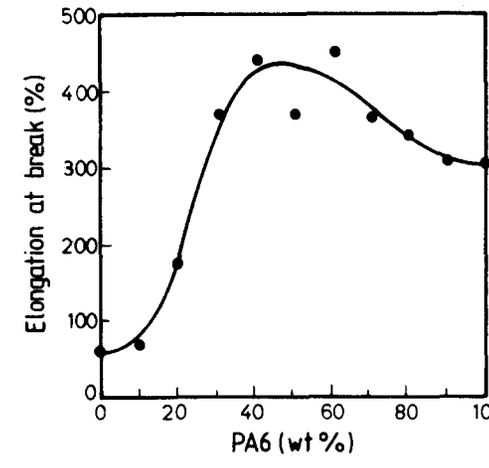

Figure 6 Elongation at break versus composition for PVDF/PA6 blends.

upon the addition of the first 40 wt% PA6 to the continuous phase of PVDF (*Figure* 2a and b). The elongation at break of pure PVDF is indeed increased by seven when 40 wt% PA6 is added.

An increase in the elongation at break that exceeds the value predicted by the mixture law could result from the combination of two favourable effects. The reduction in the yield stress observed in *Figure 5* is certainly in favour of a larger scale plastic deformation. A second effect might be associated with a higher interfacial adhesion compared to most immiscible polymer blends (at least unmodified by interfacial agents). Any improvement in the interfacial adhesion is indeed expected to delay polymer debonding at the interface and thus the initiation and propagation of voids with ultimate formation of catastrophic cracks. As a consequence, larger plastic deformation can be reached.

The beneficial effect of the PVDF/PA6 interfacial adhesion could also account for the positive deviation observed in the dependence of the ultimate tensile strength on the PA6 content (*Figure 7*). Indeed, the ultimate tensile strength of PA6 is much higher than that of PVDF, so that the continuous PVDF phase is reinforced by PA6 as efficiently as the interfacial adhesion is high. This effect allows not only for a larger plastic deformation, but also for a better orientation of the semicrystalline polymer chains before the sample is fractured.

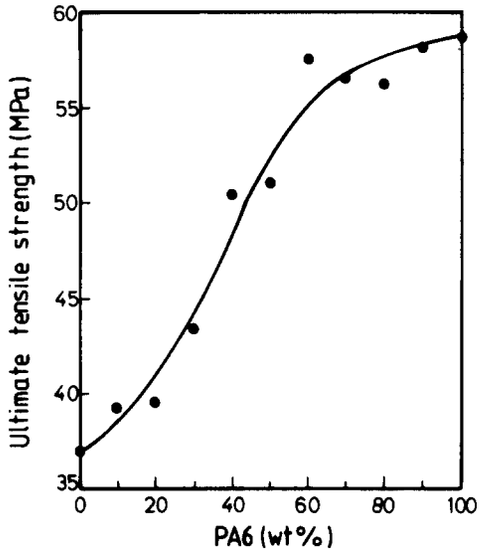

Figure 7 Ultimate tensile strength versus composition for PVDF/PA6 blends.

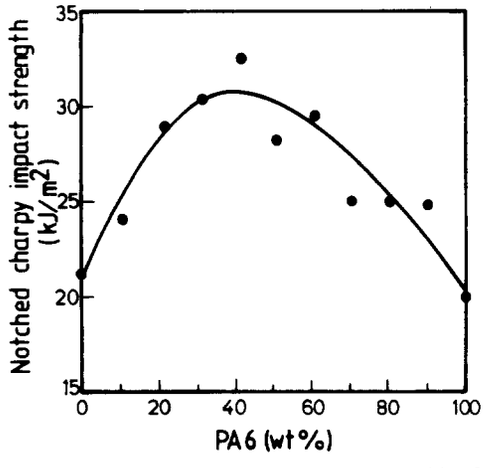

Figure 8 Notched Charpy impact strength versus composition for PVDF/PA6 blends.

The Notched Charpy impact strength shows a remarkable positive deviation that corresponds to a synergism over more than 90% of the composition range (*Figure 8*). The impact strength is known to result from a complex interplay of several experimental parameters, such as phase morphology, relative modulus of the phases, chain structure, interfacial adhesion and crystallinity, all deformation conditions being the same (temperature, rate and mode of deformation). In the present study, crystallinity, morphology and interfacial adhesion seem to be the key parameters. For instance, the decrease in crystallinity of the continuous phase results in a lower yield stress, and thus favours the matrix yielding. Moreover, nylon 6, and also PVDF to some extent, are ductile polymers (*Figure 6*), whose rubber-toughening is known to be related to the surface-to-surface interparticle distance (L) and to occur at a critical Lc value[38,39]. When $L > Lc$, the blend is brittle, whereas toughness is observed in the reverse situation ($L < Lc$). A strong adhesion is not required for toughening ductile polymers. A van der Waals adhesion seems to be strong enough, which is certainly the case in PVDF/nylon 6 blends. Nevertheless, there is no possible analogy between PVDF/nylon 6 blends with either rubber/PVDF or rubber/nylon 6 blends, even though PVDF and nylon 6 are supposed to be amorphous when they form the dispersed phase. Indeed, Tg of nylon 6 is higher than room temperature (in contrast to PVDF) and, above all, no brittle–ductile transition is observed in *Figure 8* as should be the case for the blend composition(s) at which Lc is reached when PVDF and nylon 6, respectively, is the dispersed phase. It thus appears that the impact properties of the PVDF/PA6 blends cannot be explained in a straightforward way, in reference to traditional toughening mechanism for ductile polymers. It would depend on a delicate balance between interfacial adhesion, phase morphology and crystallinity of the matrix which is still unclear. The optimization of this balance is a key strategy to trigger positive deviations, and possibly synergism, in the composition dependence of the ultimate mechanical properties (including impact) with respect to the additivity laws.

CONCLUSIONS

Although PVDF and PA6 are immiscible over the whole composition range, strong interactions occur at the interface, which accounts for a very fine phase morphology and significant improvements in the ultimate tensile strength and elongation at break compared to predictions by the additivity laws. These positive deviations, and in some composition range synergism, are also in line with a decrease in the PVDF crystallinity by the addition of PA6. The effect of the interfacial adhesion on the impact strength is complex and suggests that an optimum in the interfacial adhesion is critical for the toughening of PVDF by PA6 and synergism in this property.

ACKNOWLEDGEMENTS

The authors are grateful to the 'Services Fédéraux des Affaires Scientifiques, Techniques et Culturelles' for financial support in the frame of the 'Pôles d'Attraction Interuniversitaires: Polymères'. They also thank Professor Ph. Teyssié for his insight and encouragements in the study of 'true synergism' phenomena.

REFERENCES

1. McCarthy, R. A., *Encyclopedia of Polymer Science and Engineering*, Vol. 3, ed. J. I. Kroschwitz et al., John Wiley, New York, 1985.
2. Kawai, H., *Jap. J. Appl. Phys.*, 1969, **8**, 975.
3. Higashihata, Y., Yagi, T. and Sako, J., *Ferroelectrics*, 1986, **68**, 63.
4. Su, J., Ma, Z. Y., Scheinbeim, J. I. and Newman, B. A., *Journal of Polymer Science, Polym. Phys. Ed.*, 1995, **33**, 85.
5. Bernstein, R. E., Cruz, C. A., Paul, D. R. and Barlow, J. W., *Macromolecules*, 1977, **10**, 687.
6. Nishi, T. and Wang, T. T., *Macromolecules*, 1975, **8**, 909.
7. Paul, D. R. and Altamirano, J. O., *Adv. Chem. Ser.*, 1975, **142**, 371.
8. Mijovic, J., Luo, H. L. and Han, C. D., *Polym. Eng. Sci.*, 1982, **22**, 234.
9. Murff, S. R., Barlow, J. W. and Paul, D. R., *Adv. Chem. Ser.*, 1986, **211**, 313.
10. Ouhadi, T., Fayt, R., Jérôme, R. and Teyssié, Ph., *Journal of Polymer Science, Polym. Phys. Ed.*, 1986, **24**, 973.
11. Fayt, R., Jérôme, R. and Teyssié, Ph., *Polym. Eng. Sci.*, 1987, **27**, 328.
12. Ouhadi, T., Fayt, R., Jérôme, R. and Teyssié, Ph., *Polym. Commun.*, 1986, **27**, 212.
13. Ouhadi, T., Fayt, R., Jérôme, R. and Teyssié, Ph., *J. Appl. Polym. Sci.*, 1986, **32**, 5647.
14. Siqueira, D. F. and Nunes, S. P., *Polym. Networks Blends*, 1993, **3**, 45.
15. Deleens, G., Foy, P. and Maréchal, E., *European Polymer Journal*, 1977, **13**, 343.
16. Demont, Ph., Fourmand, L., Chatain, D. and Lacabanne, C., *Adv. Chem. Ser.*, 1990, **227**, 191.
17. Bottino, A., Capannelli, G., Munari, S. and Turturro, A., *Journal of Polymer Science, Polym. Phys. Ed.*, 1988, **26**, 785.
18. Liu, Z. H., Maréchal, Ph. and Jérôme, R., *Polymer*, 1996, **37**, 5317.
19. Matsuo, M., *Jap. Plast.*, 1968, July 6.
20. Matsuo, M., Nozaki, C. and Jyo, Y., *Polym. Eng. Sci.*, 1969, **9**, 197.
21. Wu, S., *Polymer Interface and Adhesion*, Marcel Dekker, New York, 1982.
22. Wu, S. and Chuang, H. K., *Journal of Polymer Science, Polym. Phys. Ed.*, 1986, **24**, 143.
23. Liu, Z. H., Maréchal, Ph. and Jérôme, R., *Polymer*, accepted for publication.
24. Pasztor, A. J. Jr, *Encyclopedia of Polymer Science and Engineering*, ed. J. I. Kroschwitz et al., John Wiley, New York, 1989.
25. Siqueira, D. F., Galembeck, F. and Nunes, S. P., *Polymer*, 1991, **32**, 990.
26. Wu, S., *Polym. Eng. Sci.*, 1987, **27**, 335.
27. Utracki, L. A., *J. Rheol.*, 1991, **35**, 1615.
28. Gonzalez-Montiel, A., Keskkula, H. and Paul, D. R., *Journal of Polymer Science, Polym. Phys. Ed.*, 1995, **33**, 1751.
29. Hosoda, S., Kojima, K. and Aoyagi, M., *Polym. Networks Blends*, 1991, **1**, 51.
30. Gubbels, F., Blacher, S., Vanlathem, E., Jérôme, R., Deltour, R., Brouers, F. and Teyssié, Ph., *Macromolecules*, 1995, **28**, 1559.
31. Pukanszky, P. and Tudos, F., *Makromol. Chem., Makromol. Symp.*, 1990, **38**, 221.
32. Jancar, J., Dianselmo, A. and DiBenedetto, A. T., *Polym. Eng. Sci.*, 1992, **32**, 1394.
33. Pukanszky, B., *New Polymeric Mater.*, 1992, **3**, 205.
34. Pukanszky, B., *Makromol. Chem., Macromol.Symp.*, 1993, **70/71**, 213.
35. Liu, Z. H., Ph.D. dissertation, Institute of Chemistry, Chinese Academy of Science, Beijing, 1994.
36. Kolarik, J., *Polymer*, 1994, 3631.
37. Kolarik, J., Lednicky, F., Pukanszky, B. and Pegoraro, M., *Polym. Eng. Sci.*, 1992, **32**, 886.
38. Wu, S., *Polymer*, 1985, **26**, 1855.
39. Wu, S., *J. Appl. Polym. Sci.*, 1988, **35**, 549.